


Article

Molecular Ecological Network Structure and Potential Function of the Bacterial Community in the Soil Profile under Indigenous Tree Plantations in Subtropical China

Lin Qin ^{1,*} , Yufeng Wang ¹, Angang Ming ^{2,3}, Shouhong Xi ¹, Zhirou Xiao ¹, Jinqian Teng ¹ and Ling Tan ¹

¹ Guangxi Key Laboratory of Forest Ecology and Conservation, College of Forestry, Guangxi University, Nanning 530004, China; wyf03170517@163.com (Y.W.); tengjq05@163.com (J.T.); tanlinggx@163.com (L.T.)

² Experimental Centre of Tropical Forestry, Chinese Academy of Forestry, Pingxiang 532600, China; mingangang0111@163.com

³ Guangxi Youyiguan Forest Ecosystem Research Station, Pingxiang 532600, China

* Correspondence: nilniq@gxu.edu.cn

Abstract: The soil profile is a strong and complex physicochemical gradient that greatly affects bacterial community structure and function between soil layers. However, little is known about molecular ecological network structure and bacterial community function under differing soil profiles in planted forests. Four typical native tree species (*Pinus massoniana* Lamb., *Castanopsis hystrix* Miq., *Mytilaria laosensis* Lec., and *Michelia macclurei* Dandy) plantations were selected from subtropical China as the research object. We evaluated molecular ecological network structure as well as potential function of the soil bacterial community at different soil depths (0–20, 20–40, and 40–60 cm) within native tree plantations. Our results showed that (1) compared to the topsoil (0–20 cm), the bacterial molecular ecological network scale increased within the middle layer (20–40 cm) and the subsoil (40–60 cm), and the interaction between species was stronger; (2) module hubs and connectors were the key bacterial groups in each soil layer and increased with increasing soil depth; (3) the dominant functional groups of the bacterial communities in each soil layer were chemoheterotrophy, aerobic chemoheterotrophy, cellulolysis, ureolysis, nitrogen fixation, and nitrate reduction, and they were related to soil carbon and nitrogen cycling; and (4) the different molecular ecological network structures along with relative bacterial functional group abundances among diverse soil layers were mainly affected by soil organic carbon (SOC), NO_3^- -N, NH_4^+ -N, available phosphorus (AP), and total phosphorus (TP). Our study provides a theoretical foundation for bacterial community structure together with function within soil profiles of native tree plantations in subtropical regions.

Keywords: soil bacteria; soil profile depth; molecular ecological network; FAPROTAX function prediction; subtropical plantation



Citation: Qin, L.; Wang, Y.; Ming, A.; Xi, S.; Xiao, Z.; Teng, J.; Tan, L. Molecular Ecological Network Structure and Potential Function of the Bacterial Community in the Soil Profile under Indigenous Tree Plantations in Subtropical China. *Forests* **2023**, *14*, 803. <https://doi.org/10.3390/f14040803>

Academic Editor: Julio Javier Diez

Received: 14 March 2023

Revised: 9 April 2023

Accepted: 10 April 2023

Published: 14 April 2023



Copyright: © 2023 by the authors. Licensee MDPI, Basel, Switzerland. This article is an open access article distributed under the terms and conditions of the Creative Commons Attribution (CC BY) license (<https://creativecommons.org/licenses/by/4.0/>).

1. Introduction

Soil microorganisms are the driving force of biogeochemical cycles in terrestrial ecosystems. Their functions are not limited to the surface soil and have a critical effect on deep soil [1,2]. Bacteria, the main soil microbiome components, are rich in diversity. They decompose and transform organic substances quickly and efficiently, thereby affecting plants' ability to obtain nutrients from the soil [3,4]. Previous changes in bacterial communities in soil may hamper the functioning of these communities, leading to shifts in biogeochemical cycles [5,6]. To take an example, as discovered by Xu et al. [7], some bacterial functional groups associated with carbon (C) and nitrogen (N) cycling (e.g., aerobic ammonification, nitrate reduction, chitin decomposition, etc.) changed significantly with soil depth because of altered compositions of bacterial communities between two alpine ecosystems (meadow and shrub). However, there have been many studies regarding bacterial community diversity, structure, and function in soil profiles [8,9], but the soil depth gradient response of the interaction between bacteria remains largely unclear [10,11]. Within a complex ecosystem,

interactions between species may be more crucial for ecosystem functions than species richness and diversity [12,13]. Consequently, it is significant to explore the interaction between soil bacteria in understanding the function of the terrestrial ecosystem.

In recent years, molecular ecology networks (MENs) have become the most effective analysis tool to reveal the relationship between bacteria and the relationship between bacteria and environment [14,15]. At present, there are many studies analyzing the molecular ecological networks of interspecific relations of bacterial communities in agricultural soil profiles [16]. However, few studies have been conducted to analyze molecular ecological networks for bacterial communities in forest soil, especially their structure in the forest soil profile.

Planted forests are an indispensable part of global forest resources, which have a critical effect on wood supply, ecological environment improvement, and climate change responses [17]. As demand for wood and awareness of ecological and environmental protection increase in China, large-scale afforestation and reforestation have made China's artificial forest area rank first in the world, at 79.5428 million hm^2 [18]. The change in forest management strategies from pursuing the single goal of wood production to improving the service quality and benefit of ecosystems and cultivating high-value native broadleaved forests has become the development trend in plantation management in subtropical China, which will gradually increase the area of native tree plantations [19,20]. Nonetheless, molecular ecological network structure and function for bacterial communities under the soil profiles in indigenous tree plantations in subtropical areas remain unclear.

In this study, we selected four typical native tree species (*Pinus massoniana* Lamb., *Castanopsis hystrix* Miq., *Mytilaria laosensis* Lec., and *Michelia macclurei* Dandy) as research objects of subtropical native tree plantations. *Pinus massoniana* Lamb. is one of the most important endemic coniferous timber species [21], whereas *Castanopsis hystrix* Miq., *Mytilaria laosensis* Lec., and *Michelia macclurei* Dandy are economically important native broadleaf timber species in subtropical China [22]. Based on bacterial 16S rRNA high-throughput sequencing data at diverse soil depths (0–20, 20–40, 40–60 cm) of each stand, molecular ecological network analysis and the functional annotation of prokaryotic taxa (FAPROTAX) function prediction approach were used for exploring the following scientific questions: (i) Does soil profile depth significantly affect the molecular ecological network structure as well as possible soil bacterial community function within native tree plantations? (ii) What are the dominant factors regulating the structural differences in the bacterial community molecular ecological network at soil profile depth? (iii) Are the dominant factors leading to functional differences in soil bacterial communities at various depths of the soil profile consistent with bacterial molecular ecological network structure? Insights into these questions will contribute to a theoretical basis for further understanding bacterial community structure and function in soil profiles of native tree plantations in subtropical regions.

2. Materials and Methods

2.1. Overview of the Study Site and Collection of Soil Samples

This study was carried out at the Experimental Center of Tropical Forestry of the Chinese Academy of Forestry (22°10' N, 106°50' E) in Pingxiang City, Guangxi Zhuang Autonomous Region, China. This area has a humid and semi-humid south subtropical monsoon climate with clearly separated rainy and dry seasons. The yearly rainfall can be about 1400 mm, which mostly occurs during the rainy season that extends from April to September; the yearly average temperature reaches 21 °C, and the average monthly maximal and minimal temperatures are 26.3 and 12.1 °C, respectively. Its topography primarily includes low hills and mountains (altitude, 430–680 m). The soil mainly contains red soil in line with Chinese soil classification, which is the same as oxisol in the USDA Soil Taxonomy. The soil thickness is generally greater than 80 cm [21,23].

In August 2016, four pure plantations (*Pinus massoniana* Lamb., *Castanopsis hystrix* Miq., *Mytilaria laosensis* Lec., and *Michelia macclurei* Dandy) with similar site conditions (soil type, altitude, slope, and aspect) and the same management measures were selected.

Four artificial pure forests were planted (density: 2500 plants/hm²) on the cutting site of a *Cunninghamia lanceolata* (Lamb.) Hook. plantation. The *Pinus massoniana* Lamb. and *Castanopsis hystrix* Miq. plantations were created in 1983, whereas *Mytilaria laosensis* Lec. and *Michelia macclurei* Dandy plantations were created in 1981. This experiment set up three plots of 20 m × 20 m on every stand; intervals between plots were at least 20 m. For every plot, we chose three sampling sites at random along the left diagonal, and soil samples from the topsoil (0–20 cm), middle layer (20–40 cm), and subsoil (40–60 cm) were collected with a soil drill (5.0 cm in inner diameter). After removing impurities such as animal and plant residues and stones, the soil samples from the same layer were blended for forming the mixed sample and placed in a sterile sampling bag, which was stored in a biological ice bag before being brought to the laboratory. Fresh mixed samples were divided into three batches in the laboratory. The first batch of fresh soil samples was immediately stored in a −80 °C refrigerator after passing through a 2 mm steel sieve, for high-throughput sequencing of soil bacteria. The second batch was immediately stored in a 4 °C refrigerator after passing through a 2 mm steel sieve, for ammonium and nitrate nitrogen content detection. The third part was dried with indoor natural air and passed through a 0.25 mm sieve for determining soil physicochemical characteristics.

2.2. Soil Physicochemical Characteristic Measurement

We analyzed soil water content (SWC) according to Lu [24] and measured soil pH value with potentiometry (water-to-soil ratio of 2.5:1, *v/w*) (PHS-3C laboratory pH meter, Shanghai Jinhuan Instrument Co., LTD, Shanghai, China). Additionally, the potassium dichromate oxidation method was adopted to analyze soil organic carbon (SOC) concentration, whereas an automatic chemical analyzer (Smartchem200, Alliance, Paris, France) was used for analyzing total nitrogen (TN) concentration following digestion with concentrated sulfuric acid and perchloric acid. Additionally, an automatic chemical analyzer (Smartchem 200, Alliance, France) was utilized to determine nitrate nitrogen (NO₃[−]-N) and ammonium nitrogen (NH₄⁺-N) levels following alkali solution diffusion and calcium sulfate leaching. Sodium hydroxide alkali melting-molybdenum–antimony resistance colorimetry [24] was utilized for determining total phosphorus (TP) content, and the available phosphorus (AP) content was determined with an automatic chemical analyzer (Smartchem 200, Alliance, Paris, France) following double acid leaching.

2.3. Isolation of Soil Bacterial DNA, PCR Amplification, and High-Throughput Sequencing (HTS)

By adopting the PowerSoil[®] DNA Isolation Kit (Mo Bio Laboratories Inc., Carlsbad, CA, USA), we isolated soil bacterial DNA. UV–Vis spectrophotometry (Thermo Nano-Drop 2000, Thermo Fisher Scientific, Waltham, MA, USA) as well as 1.2% agarose gel electrophoresis (AGE) was conducted to verify total DNA quality. Universal primers 515F (5′-GTGCCAGCMGCCGCGGTAA-3′) and 926R (5′-CCGTCAATTCMTTGTAGTTT-3′) were utilized for amplifying the bacterial 16S rRNA gene V4–V5 region.

The gene library was constructed using PCR amplification in two steps. The first PCR amplification reaction volume consisted of 5 × buffer (10 µL), dNTP (1 µL, 10 mmol/L), F/R inner primers (1 µL, 10 µmol/L), 1U Phusion high-fidelity DNA polymerase, and 5–50 ng DNA template, topped up to 50 µL with ddH₂O. The reaction was carried out under the following conditions: 2 min under 94 °C, 25 × (30 s under 94 °C, 30 s under 56 °C, and 30 s under 72 °C), and 5 min under 72 °C. Then, 2% AGE was conducted to confirm PCR products, followed by recovery with the AxyPrep DNA gel extraction kit (AXYGEN Axygen Scientific Inc., San Francisco, CA, USA) for second PCR amplification comprising 5 × buffer (8 µL), dNTP (1 µL, 10 mmol/L), Phusion high-fidelity DNA polymerase (0.8 U), F/R inner primers (1 µL, 10 µmol/L) each, and 5 µL DNA template, topped up to 40 µL with ddH₂O. The reaction conditions for the second amplification were 94 °C for 2 min, 8 × (30 s under 94 °C, 30 s under 56 °C, and 30 s under 72 °C), as well as 5 min under 72 °C. Later, 2% AGE was conducted to verify PCR products, followed by recovery using the AxyPrep DNA gel extraction kit (Axygen Scientific Inc., San Francisco, CA, USA).

as well as quantification through FTC-3000™ RT-PCR. Gene library construction was completed by mixing the PCR products. Illumina MiSeq (TinyGene Bio-Tech (Shanghai) Co., Ltd., Shanghai, China) was adopted for HTS of the 16S rRNA at a 2×300 bp read length. The 16S rRNA gene sequencing data were deposited in NCBI SRA with BioProject ID PRJNA 886117.

2.4. Bioinformatic Analysis

According to the barcode obtained with the Illumina platform sequencing, PE was read to distinguish each sample; the sequence quality was controlled and filtered. Quality control of effective sequences was performed using Trimmomatic software. The alignment of effective sequences was completed using FLASH software (Version 1.2.11, Johns Hopkins University, Baltimore, MD, USA). Later, we aligned paired reads to one sequence based on overlapping regions among the PE reads, with the minimal overlapping length of 10 bp and a 0.2 maximal mismatch ratio within aligned sequence overlapping areas. Optimized sequences were obtained by filtering out singletons from the aligned long reads using the software package Mothur (Version 1.33.3, Ann Arbor, MI, USA).

Next, we clustered optimal sequences into operational taxonomic units (OTUs) with the USEARCH software package. Briefly, the optimized sequences were clustered at 97% similarity for obtaining typical OTU sequences using UPARSE. Subsequently, UCHIME was utilized to eliminate PCR amplification-derived chimeras from the representative OTU sequences. Finally, the Greengene (Release 13.5, <http://greengenes.secondgenome.com/>, accessed on 17 October 2018) database was used to compare typical OTU sequences acquired for species annotation (confidence threshold = 0.8) using Mothur (classify.seqs).

The establishment of bacterial molecular ecological networks was based on OTU information [14]. Logarithmically transformed (\log_{10}) OTU data were used for calculating Pearson correlations of any two OTUs by using the MENA platform (<http://ieg4.rccc.ou.edu/MENA>, accessed on 23 April 2021). By adopting random matrix theory (RMT), this step built a bacterial molecular ecological network, followed by calculation of network topology parameters, including network nodes, edges, average clustering coefficient, average degree, modularity and average path distance [25,26]. According to the node intra- and inter-module connectivity (Z_i and P_i , respectively), all nodes within the network were classified into four types [27]: (i) module hub ($Z_i \geq 2.5$, $P_i < 0.62$); (ii) connector ($Z_i < 2.5$, $P_i \geq 0.62$); (iii) network hub ($Z_i \geq 2.5$, $P_i \geq 0.62$); and (iv) peripheral nodes ($Z_i < 2.5$, $P_i < 0.62$). For molecular ecological networks, network hubs, module hubs, and connectors have usually been considered key species [27]. This study visualized molecular ecological network structure using Cytoscape v3.7.1 (<http://manual.cytoscape.org/en/stable/>, accessed on 25 April 2021).

Functional annotation of prokaryotic taxa (FAPROTAX) can be used for predicting bacterial community functions based on OTU data of 16S rRNA, which mainly include over 7600 functional annotations in over 80 functional groups (such as methanogenesis, nitrate respiration, plant pathogens, and fermentation) obtained in at least 4600 prokaryotes [28]. FAPROTAX has become an analytical tool for studying the biogeochemical cycle and key bacterial functions of bacteria–bacteria and plant–bacteria interactions [29]. The functional groups of the bacterial communities within native plantation soil profiles were analyzed with the FAPROTAX platform (<http://www.loucalab.com/archive/FAPROTAX/>, accessed on 20 June 2021).

2.5. Statistical Analysis

This study utilized one-way analysis of variance (ANOVA) for detecting significance of differences in physicochemical characters of soils and functional groups of dominant bacteria among different soil layers, followed by Tukey's HSD multiple comparisons, which were carried out with SPSS (Version 24.0, IBM, Chicago, IL, USA). Hierarchical clustering was employed to cluster the representative bacterial molecular ecological network modules, and Pearson correlation coefficients were utilized for analyzing association of

soil physicochemical characters with representative modules (module characteristic OTU) within the same soil layer. These calculations were completed with the MENA platform (<http://ieg4.rccc.ou.edu/MENA>, accessed on 23 April 2021). We used the Pearson correlation coefficient to determine which physicochemical factors were associated with the soil bacterial community functional groups.

3. Results

3.1. Alterations of Soil Physicochemical Character in Native Tree Plantations

The SWC, SOC, TN, NO_3^- -N, NH_4^+ -N, AP, and TP of native tree plantations declined as soil depth increased (Table 1). Topsoil SWC remarkably increased compared with the other two soil layers ($p < 0.05$), but the middle layer was not significantly different compared with the subsoil ($p > 0.05$). SOC, TN, and NO_3^- -N significantly differed among the three soil layers. Topsoil NH_4^+ -N was remarkably elevated within the subsoil; however, the middle layer was not significantly different compared with the topsoil and subsoil. TP in the topsoil and middle layer did not exhibit any significant difference, but both were remarkably elevated compared with the subsoil. The different amounts of AP among the three soil layers were not significant.

Table 1. Changes in physicochemical properties of soil profiles in native tree plantations (mean \pm SD, $n = 12$).

Soil Layer	SWC (%)	pH	SOC (g/kg)	TN (g/kg)	NH_4^+ -N (mg/kg)	NO_3^- -N (mg/kg)	TP (g/kg)	AP (mg/kg)
0–20 cm	31.32 \pm 2.56 a	4.17 \pm 0.24 a	21.17 \pm 2.11 a	1.43 \pm 0.34 a	19.38 \pm 5.49 a	4.42 \pm 0.63 a	1.26 \pm 0.49 a	13.85 \pm 3.64 a
20–40 cm	28.02 \pm 2.92 b	4.23 \pm 0.31 a	12.05 \pm 1.87 b	1.10 \pm 0.20 b	15.07 \pm 7.09 ab	3.20 \pm 1.06 b	0.96 \pm 0.44 a	11.76 \pm 4.98 a
40–60 cm	25.86 \pm 3.69 b	4.27 \pm 0.25 a	9.58 \pm 1.62 c	0.74 \pm 0.17 c	10.07 \pm 6.37 b	1.93 \pm 0.87 c	0.43 \pm 0.22 b	9.99 \pm 5.27 a

SWC: soil water content; SOC: soil organic carbon; TN: total nitrogen; NH_4^+ -N: ammoniacal nitrogen; NO_3^- -N: nitrate nitrogen; TP: total phosphorus; AP: available phosphorus. Different lowercase letters represent significant differences among the different soil layers at a level of 0.05.

3.2. Characteristics of Bacterial Molecular Ecological Network Structure within Soil Profiles of Native Tree Plantations

The network topology parameters showed that the threshold value for the soil bacterial molecular ecological network in three soil layers was 0.760, and R^2 of the power law was around 0.8 (Table 2), in line with the power law [13]. Additionally, average path distance and average clustering coefficient, together with the modularity index for the bacterial molecular ecological network in each soil layer increased compared with those in a random network, which indicated that these three bacterial molecular ecological networks built in this study conform to basic network features, including small world, scale-free, and modular [13].

Topological parameters for the soil bacterial molecular ecological network among the three soil layers showed that the total links, total nodes, and average clustering coefficients were as follows: topsoil < middle layer < subsoil. The average degree was as follows: topsoil < subsoil < middle layer, and the average path distance and modularity index were topsoil > subsoil > middle layer (Table 2 and Figure 1). Meanwhile, the positive connections for the soil bacterial molecular ecological network within the topsoil, middle layer, and subsoil accounted for 78.98%, 70.70%, and 66.28% of the total edges, respectively.

Table 2. Topological parameters of molecular ecological networks and random network of the bacterial community in the soil profiles of native tree plantations.

Soil Layer	Molecular Ecological Networks							Random Networks					
	Cutoff	Total Nodes	Total Links	R ² of Power Law	The Number of Positive Connections	The Number of Negative Connections	Average Degree	Average Clustering Coefficient	Average Path Distance	Modularity Index (Module Number)	Average Clustering Coefficient	Average Path Distance	Modularity Index
0–20 cm	0.76	166	333	0.752	263	70	4.012	0.203	4.451	0.669 (16)	0.029 ± 0.009	3.665 ± 0.051	0.475 ± 0.009
20–40 cm	0.76	191	488	0.813	345	143	5.11	0.225	4.148	0.586 (15)	0.049 ± 0.009	3.308 ± 0.043	0.400 ± 0.007
40–60 cm	0.76	204	519	0.796	344	175	5.088	0.235	4.204	0.623 (12)	0.042 ± 0.008	3.359 ± 0.035	0.406 ± 0.007

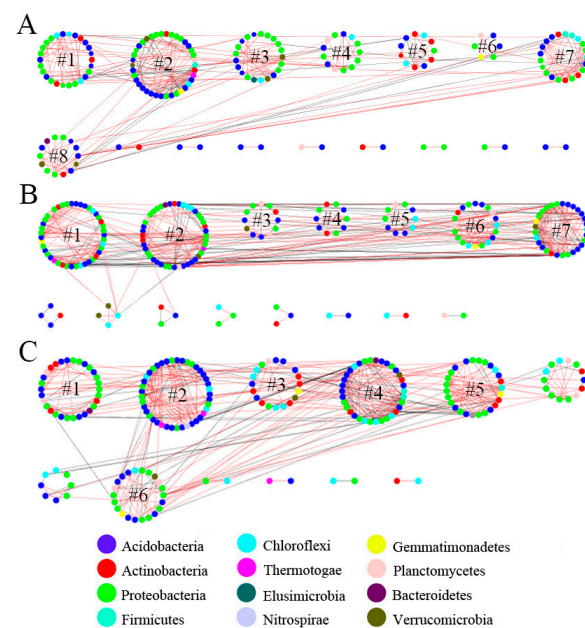


Figure 1. The molecular ecological network of soil bacteria in the topsoil (0–20 cm) (A), middle layer (20–40 cm) (B), and subsoil (40–60 cm) (C) of native tree plantations. Each node represents an OTU of bacteria, and the color of the node represents the phylum level of bacteria. The red line indicates the positive interaction between nodes, and the gray line indicates the negative interaction between nodes. # k , Module k , $k = 1, 2, 3, \dots$.

3.3. Topological Functions of Bacterial Molecular Ecological Network Nodes within Soil Profiles of Native Tree Plantations

The soil bacterial molecular ecological network (OTU level) showed 268 non-repeating nodes in the three soil layers (Figure 2). Among them, there were 109 shared nodes in the three soil layers and 15, 24 and 45 unique nodes in the surface, middle, and bottom layers, respectively. Further statistics revealed that peripheral nodes were dominant in all soil layers (topsoil: 98.80%; middle level: 96.34%; subsoil: 92.65%) without network hubs (Figure 3). There were two key nodes on the soil surface, one module hub, and one connector, that belonged to Actinobacteria and Firmicutes, respectively (each accounting for 50.00%) (Figures 3 and 4A). There were seven key nodes in the middle layer, including two module hubs and five connectors, belonging to four bacterial phyla, of which Proteobacteria accounts for the largest proportion (42.86%), followed by Planctomycetes (28.57%); Chloroflexi was the key endemic bacteria (Figures 3 and 4B). There were fifteen key nodes in the subsoil, including three module hubs and twelve connectors that belonged to six bacterial phyla: Proteobacteria (26.67%), Acidobacteria (26.67%), Actinobacteria (20.00%), Planctomycetes (13.33%), Firmicutes (6.67%), and Verrucomicrobia (6.67%) (Figures 3 and 4C).

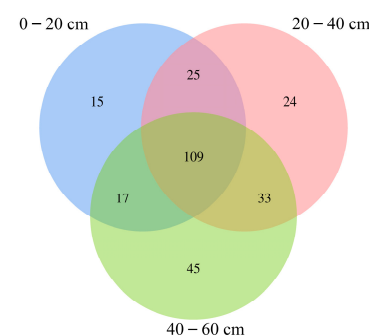


Figure 2. Venn diagram of node distribution of bacterial molecular ecological network in three soil layers.

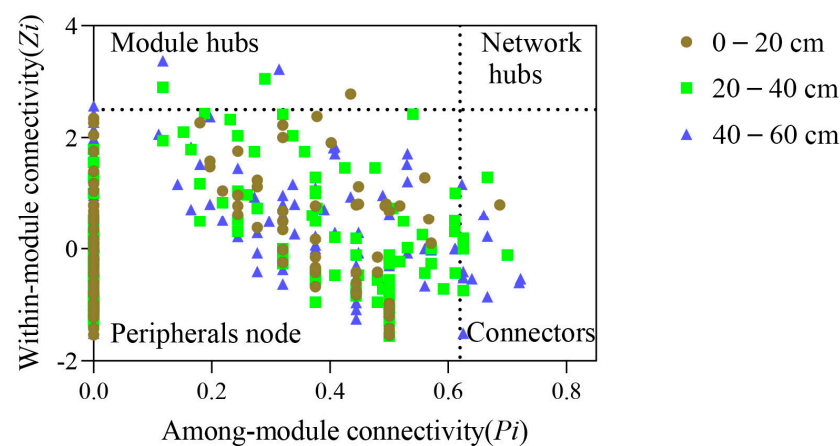


Figure 3. Topological role distribution of bacterial molecular ecological network nodes in three soil layers.

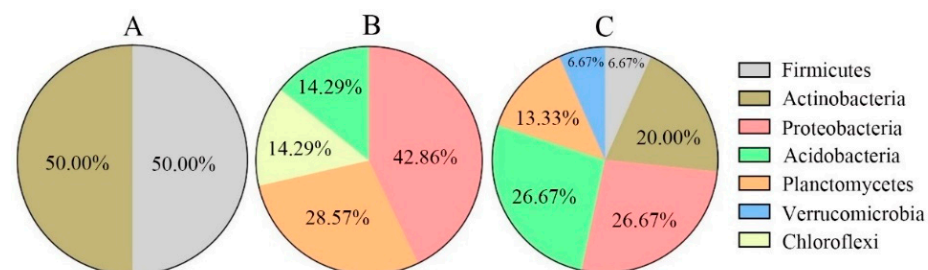


Figure 4. Distribution patterns of key phylum in topsoil (A), middle layer (B), and subsoil (C) of native tree plantation.

3.4. Functions of Soil Physicochemical Characteristics in Bacterial Molecular Ecological Network Structure

From the view of the module hierarchy among the bacterial molecular ecological networks in each soil layer, modules 1 and 3 were closely related; modules 5 and 6 were closely related; modules 4, 7, and 8 were closely related; and module 2 was different from the other modules in the topsoil (Figure 5(A1)). Modules 2, 4, and 7 were closely linked; modules 1 and 5 were closely linked; and modules 3 and 6 were closely linked in the middle layer (Figure 5(B1)). Modules 2 and 5 were closely connected; modules 3, 4, and 6 were closely connected; and module 1 was distinctly different from the other modules in the subsoil (Figure 5(C1)).

The effects of physicochemical characteristics of soil on bacterial molecular ecological network structure were different among different soil layers. In the topsoil, $\text{NH}_4^+\text{-N}$ showed a significantly positive relation to module 8 ($r = 0.62$, $p < 0.05$), whereas TP showed a significantly positive relation to module 6 ($r = 0.68$, $p < 0.05$) and module 7 ($r = 0.65$, $p < 0.05$) (Figure 5(A2)). In the middle layer, AP showed a significantly positive relation to module 7 ($r = 0.63$, $p < 0.05$), whereas SOC showed a significantly positive relation to module 4 ($r = 0.62$, $p < 0.05$), together with module 6 ($r = 0.58$, $p < 0.05$) (Figure 5(B2)). In the subsoil, $\text{NO}_3^-\text{-N}$ showed a significantly negative relation to module 2 ($r = -0.7$, $p < 0.05$), while SOC showed a significantly positive relation to module 1 ($r = 0.58$, $p < 0.05$) (Figure 5(C2)). Overall, SOC, $\text{NO}_3^-\text{-N}$, $\text{NH}_4^+\text{-N}$, AP, and TP accounted for dominant parameters that affected bacterial molecular ecological network structure within the soil profile.

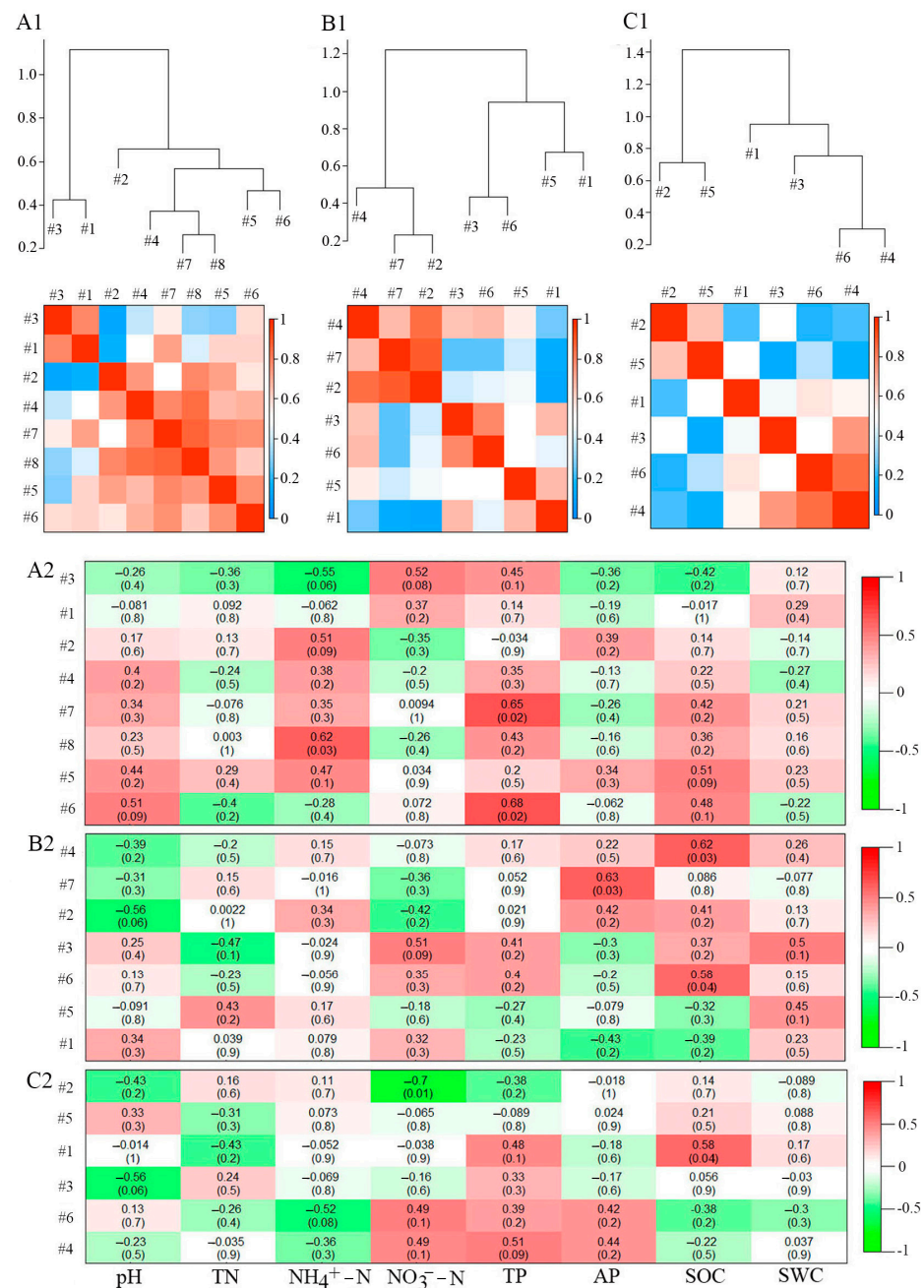


Figure 5. Hierarchical structure of three soil bacterial molecular ecological network modules and its correlation with soil physical and chemical properties. (A1,B1,C1) represent the hierarchical structure diagram and heat diagram of representative modules of soil bacterial molecular ecological network in the topsoil, middle layer, and subsoil, respectively. Among them, the upper part was the hierarchical clustering structure diagram based on the Pearson correlation between representative modules, and the lower part was the heat map based on the Pearson correlation between representative modules. Red indicates a high correlation, and blue indicates a low correlation. (A2,B2,C2) represent the correlation heat map between the representative modules of soil bacterial molecular ecological network and soil physicochemical properties in the topsoil, middle layer, and subsoil, respectively. In those figures, red indicates a high positive correlation, and green indicates a high negative correlation. In each figure, the numbers without brackets and those with brackets represent correlation coefficient (r) and significance (P), respectively. # k , Module k , $k = 1, 2, 3, \dots$. SWC: soil water content; SOC: soil organic carbon; TN: total nitrogen; $\text{NH}_4^+\text{-N}$: ammoniacal nitrogen; $\text{NO}_3^-\text{-N}$: nitrate nitrogen; TP: total phosphorus; AP: available phosphorus.

3.5. FAPROTAX Bacterial Functional Estimation within the Soil Profile in Native Tree Plantations

Results of soil bacterial community functional group annotation showed that the number of functional groups of the topsoil, middle layer, and subsoil were 43, 46, and 46, respectively, and the relative abundances of identified OTUs were 65.1426%, 55.6798%, and 58.5035%, respectively (Table 3). Based on a relative abundance greater than 0.5% in each soil layer, the six dominant functional groups of the soil bacterial community were determined as follows: chemoheterotrophic, aerobic chemoheterotrophic, cellulolysis, urea hydrolysis, nitrogen fixation, and nitrate reduction. ANOVA revealed that different soil layers were not significantly different in chemoheterotrophic, aerobic chemoheterotrophic, cellulolysis, nitrogen fixation, and nitrate reduction ($p > 0.05$). Urea hydrolysis within topsoil was remarkably elevated compared with the middle layer and subsoil ($p < 0.05$), but the latter two were not significantly different ($p > 0.05$) (Figure 6).

Table 3. Relative abundance of bacterial functional groups in the soil profile of native tree plantations.

Bacterial Functional Group	Relative Abundance (%)		
	0–20 cm	20–40 cm	40–60 cm
chemoheterotrophy	26.3037	21.6669	21.7211
aerobic chemoheterotrophy	25.8136	21.1417	21.2079
cellulolysis	4.3823	4.9789	4.3766
ureolysis	5.1485	2.7107	2.8567
nitrogen fixation	0.5692	0.6592	0.8078
nitrate reduction	0.6468	0.5049	0.7700
methanotrophy	0.0115	0.0199	0.0178
methanol_oxidation	0.0191	0.0444	0.0738
methylo trophy	0.0306	0.0643	0.0916
aerobic_ammonia_oxidation	0.0011	0.0010	0.0022
aerobic_nitrite_oxidation	0.0146	0.0979	0.2692
nitrification	0.0157	0.0989	0.2714
sulfur_respiration	0.0000	0.0006	0.0015
respiration_of_sulfur_compounds	0.0000	0.0006	0.0015
chitinolysis	0.0004	0.0002	0.0002
nitrite_ammonification	0.0938	0.2136	0.3710
nitrite_respiration	0.0938	0.2136	0.3710
dark_thiosulfate_oxidation	0.0731	0.0210	0.0135
dark_oxidation_of_sulfur_compounds	0.0736	0.0212	0.0135
manganese_oxidation	0.0086	0.0119	0.0175
fermentation	0.2850	0.3708	0.5907
invertebrate_parasites	0.0017	0.0021	0.0038
human_pathogens_pneumonia	0.0000	0.0012	0.0013
human_pathogens_gastroenteritis	0.0938	0.2136	0.3710
human_pathogens_diarrhea	0.0938	0.2136	0.3710
human_pathogens_all	0.1186	0.2504	0.4334
human_gut	0.0946	0.2136	0.3724
human_associated	0.1195	0.2504	0.4349
mammal_gut	0.0946	0.2136	0.3724
animal_parasites_or_symbionts	0.2356	0.3761	0.5379
plant_pathogen	0.0570	0.0292	0.0433
aromatic_hydrocarbon_degradation	0.0006	0.0014	0.0021
aromatic_compound_degradation	0.0336	0.0665	0.1346
liphatic_non_methane_hydrocarbon_degradation	0.0006	0.0014	0.0021
hydrocarbon_degradation	0.0121	0.0214	0.0199
iron_respiration	0.0304	0.0455	0.0482
nitrate_respiration	0.1117	0.2414	0.4375

Table 3. Cont.

Bacterial Functional Group	Relative Abundance (%)		
	0–20 cm	20–40 cm	40–60 cm
nitrogen_respiration	0.1117	0.2414	0.4375
fumarate_respiration	0.0938	0.2136	0.3710
intracellular_parasites	0.1295	0.1084	0.0770
predatory_or_exoparasitic	0.0368	0.0438	0.0694
chloroplasts	0.0045	0.0103	0.0084
nonphotosynthetic_cyanobacteria	0.0382	0.0210	0.0239
aerobic_anoxygenic_phototrophy	0.0010	0.0006	0.0051
photoheterotrophy	0.0219	0.0287	0.0393
phototrophy	0.0219	0.0287	0.0393
Total	65.1426	55.6798	58.5035

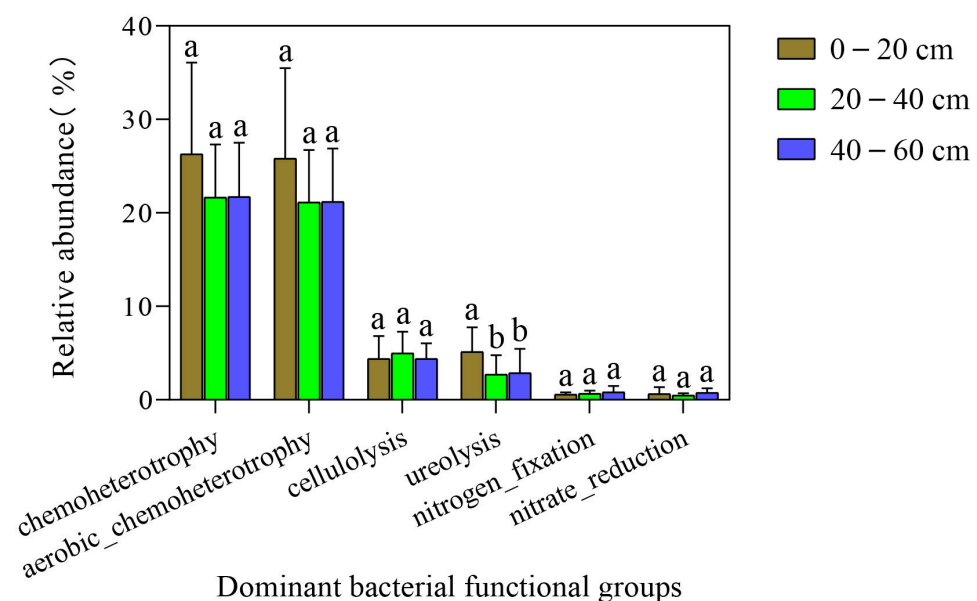


Figure 6. Comparison of relative abundance of the six dominant bacterial functional groups in soil profiles of native tree plantations. Different lowercase letters represent significant differences among different soil layers at 0.05 level.

Pearson correlation analysis further showed that soil physicochemical properties had different effects on the dominant bacterial functional groups in each soil layer (Figure 7). In the topsoil, chemoheterotrophic and aerobic chemoheterotrophs were significantly positively correlated with soil TP ($p < 0.05$), and cellulolysis was significantly positively correlated with soil pH and SOC ($p < 0.05$) (Figure 7A). In the middle layer, chemoheterotrophic, aerobic chemoheterotrophic, and nitrate reduction were significantly positively correlated with SOC ($p < 0.05$); nitrate reduction, nitrogen fixation, and urea hydrolysis were significantly positively correlated with soil $\text{NH}_4^+\text{-N}$ ($p < 0.05$); and nitrogen fixation was significantly negatively correlated with $\text{NO}_3^-\text{-N}$ ($p < 0.05$) (Figure 7B). Subsoil nitrogen fixation was significantly and positively correlated with AP ($p < 0.05$) (Figure 7C). Overall, soil pH, SOC, $\text{NH}_4^+\text{-N}$, $\text{NO}_3^-\text{-N}$, TP, and AP were the dominant factors affecting the dominant functional groups of the bacterial communities in the soil profile.

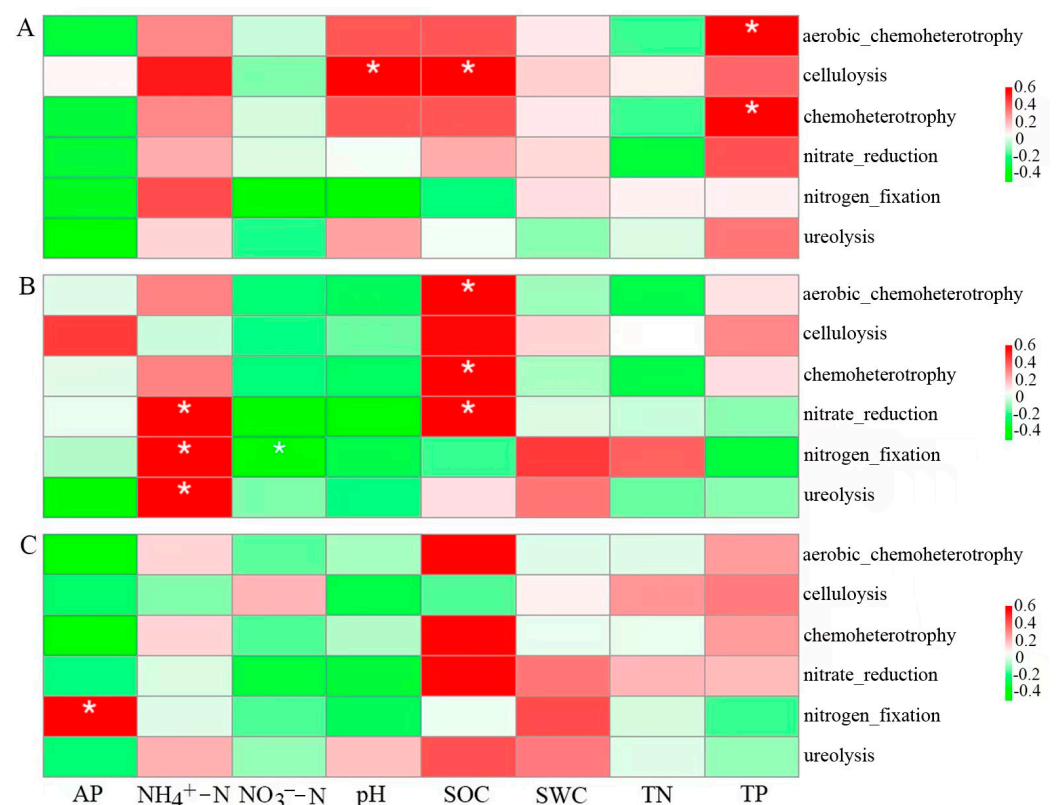


Figure 7. Correlation between the six dominant bacterial functional groups and soil physicochemical properties in topsoil (A), middle layer (B), and subsoil (C). * $p < 0.05$. SWC: soil water content; SOC: soil organic carbon; TN: total nitrogen; NH₄⁺-N: ammoniacal nitrogen; NO₃⁻-N: nitrate nitrogen; TP: total phosphorus; AP: available phosphorus.

4. Discussion

4.1. Function of Soil Profile Depth in Bacterial Molecular Ecological Network Structure

We found that edge and numbers, along with negative connections of soil bacterial molecular ecological networks within native tree plantations increased with increasing soil depth (Table 2 and Figure 1), which indicated a larger soil bacterial molecular ecological network scale [25] and stronger competition among subsoil bacteria [30]. Mundra et al. showed that numbers of negative connections of soil bacterial molecular ecological networks in *Betula pubescens* forests in Norway increased with increasing soil depth [31], conforming to our findings. The reason may be that nutrients (SWC, SOC, TN, NO₃⁻-N, NH₄⁺-N, AP and TP) decreased with increasing soil depth (Table 1), resulting in relatively limited nutrients in the subsoil, promoting the succession of bacterial communities with more efficient nutrient utilization efficiency [32,33]. Competition between bacteria is reduced in soils with relatively abundant nutrients [34], whereas bacteria need to meet their own needs through stronger competition in relatively scarce resources [35].

Average connectivity and clustering coefficient represent the molecular ecological network complexity and community organization order, respectively. The above indexes in the middle layer and subsoil in native tree plantations significantly increased compared with topsoil, which suggested a more complex and organized bacterial molecular ecological network and community organization in the middle and subsoil layers than those in the topsoil (Table 2 and Figure 1). Xu et al. revealed that the average clustering coefficient of topsoil (0–20 cm) in a Tibetan Plateau meadow was lower than that of subsoil (30–70 cm) [7]. Further, these two indices of farmland elevated with an increase in soil depth in Tianjin, China [16]. These results were consistent with those of this study.

Network average path distance represents the matter/energy/information transfer efficiency between the species. A smaller average path distance indicates greater matter/energy/information transfer efficiency between species; however, the response to disturbance is also more sensitive. The modularity index is a measure of the degree of modularity of a network structure and is commonly used to represent the system's resistance to external interference. The higher the modularity index, the stronger the resistance to external interference [25]. According to our results, for the bacterial molecular ecological network, average path distance and modularity index in the topsoil of native tree plantations were significantly greater than those in the middle layer and subsoil (Table 2 and Figure 1), conforming to the study by Bai et al. [36] on the modularity index of bacterial network structure in paddy soil, indicating that topsoil bacterial community structure remained relatively stable when the external environment changed; however, the bacterial community structure in the other two soil layers was easily disturbed.

Module connectors and hubs represent the key species during community composition and have a critical effect on keeping community structural stability [27]. Their removal can cause significant changes in structures and functions of bacterial communities [37]. In this study, we found that the modular hubs and connectors of soil bacteria networks on plantations increased with increasing soil depth (Figure 3), indicating the relative stability of topsoil bacterial communities. However, more modular hubs and connectors were needed in the middle and bottom layers for maintaining bacterial community structural stability. Meanwhile, Firmicutes and Actinobacteria represented key phyla within the topsoil; Proteobacteria, Planctomycetes, Acidobacteria, and Chloroflexi within middle layer; and Proteobacteria, Acidobacteria, Actinobacteria, Planctomycetes, Firmicutes, and Verrucomicrobia within the subsoil (Figure 4). This is because Firmicutes, Actinobacteria, Proteobacteria, and Acidobacteria were relatively abundant in each soil layer (Figure 4) and were more likely to survive under environmental interference and participate in constructing the molecular ecological network structure [38]. Additionally, different types of bacteria have varied life forms and functions. For example, Acidobacteria have a slow metabolism and easily become key species when their living environment is affected. They are all important participants in biochemical cycling processes such as carbon and nitrogen cycling in the soil. Firmicutes can improve the phosphorus content in the soil as phosphate-solubilizing bacteria and participate in nitrogen fixation [39] and have an important effect on lignocellulose degradation [40]. Actinobacteria are often involved in the degradation of some stable polymer compounds, such as lignin and cellulose, and also have a crucial effect on soil carbon source decomposition [41,42]. Chloroflexi promote starch degradation and accelerate the anti-interference ability of functions related to the carbon cycle [43].

Soil physicochemical characteristics such as soil carbon, nitrogen, and phosphorus content are the main energy sources and nutrients of soil bacteria [44] and are also key factors that regulate different structures of soil bacterial communities among different soil layers [45]. This study found that soil $\text{NH}_4^+\text{-N}$ and TP were critical factors that affect topsoil bacterial molecular ecological network structure, while SOC and AP were the key factors affecting the bacterial molecular ecological network structure within the middle layer; additionally, SOC and $\text{NO}_3^-\text{-N}$ accounted for critical factors that affected subsoil bacterial molecular ecological network structure (Figure 5). Based on the results, bacterial molecular ecological network structures among different soil layers were significantly affected by soil physicochemical characteristics such as SOC, $\text{NO}_3^-\text{-N}$, $\text{NH}_4^+\text{-N}$, TP, and AP, partially conforming to earlier observations from subtropical broadleaved forests [46] and dryland-to-paddy conversion [47] in China.

4.2. Function of Soil Profile Depth in Soil Bacterial Community Function

Soil bacteria represent soil microbial groups with the highest complexity and diversity, whose potential functions are crucial for forest productivity [48]. They can directly participate in a variety of ecosystem service processes related to biogeochemical cycles, including carbon and nitrogen cycles [49]. In this study, chemoheterotrophy and aerobic heterotrophy

had the highest abundance in each soil layer, indicating that numerous bacteria obtain energy and carbon by means of soil organic matter decomposition [50,51]. Pearson correlation analysis further found that chemoheterotrophy and aerobic heterotrophy showed a markedly positive relation to SOC ($p < 0.05$), indicating that alterations of the soil carbon pool is the possible major factor driving soil bacterial functional group function [52]. In addition, cellulolysis was markedly positively related to soil pH ($p < 0.05$), indicating that an increase in soil pH could improve the abundance of cellulolysis and hence, promote carbon cycling. Liang et al. found that the soil pH of different land use modes (natural secondary forest, shrub, coniferous forest, pine, and farmland) had a significant impact on the cellulose hydrolysis type among eastern mountain regions in Liaoning province, China [53], conforming to our findings.

More than 80% of global nitrogen emissions can be attributed to soil microbial activity [54], mainly soil bacteria-mediated soil nitrogen cycles, including aerobic nitrification and anaerobic denitrification [55]. In this study, the three dominant functional groups (ureolysis, nitrogen fixation, nitrate reduction) were involved in soil nitrogen cycling (nitrogen fixation, nitrification, denitrification, etc.). Ureolysis was significantly different among the topsoil, middle layer, and subsoil ($p < 0.05$), but the middle layer was not significantly different from subsoil ($p > 0.05$). Nitrogen fixation and nitrate reduction were not significantly different in each soil layer ($p > 0.05$). Xu et al. found that ureolysis of shrubs in the Tibetan Plateau changed significantly depending on soil profile ($p < 0.05$), while nitrate reduction did not exhibit any significant difference in all soil layers ($p > 0.05$) [7], conforming to our findings. Pearson correlation analysis further found that nitrogen fixation, ureolysis, and nitrate reduction were significantly correlated with SOC, $\text{NH}_4^+\text{-N}$, $\text{NO}_3^-\text{-N}$, and AP. Previous studies have also shown various soil physicochemical characteristics (e.g., SOC, pH, $\text{NH}_4^+\text{-N}$, and $\text{NO}_3^-\text{-N}$) significantly affected the soil bacteria-driven N cycle process [53].

Overall, this study only discussed the molecular ecological network structure and potential function of a bacterial community in the soil profile of forest plantations in summer and could not reflect the effect of seasonal changes on the structure and function of the soil bacterial community.

5. Conclusions

The soil bacterial molecular ecological network structure experienced remarkable changes owing to variation in soil chemical properties in subtropical native plantations. The molecular ecological network structure in middle and bottom soil layer bacteria displayed increased complexity compared with topsoil, and the interactions between bacteria were strong. The dominant functional groups of the bacteria involved in carbon and nitrogen cycling in each soil layer were chemoheterotrophy, aerobic chemoheterotrophy, cellulolysis, nitrogen fixation, ureolysis, and nitrate reduction. SOC, $\text{NO}_3^-\text{-N}$, $\text{NH}_4^+\text{-N}$, AP, and TP accounted for major factors that regulated differences in molecular ecological network structure and dominant bacterial functional group abundances among the diverse soil layers. Future studies may focus on the effects of seasonal variation on the molecular ecological network structure and potential function of the soil bacterial community under the planted forests in this region, which will contribute to a comprehensive understanding of the structure and function of the soil bacterial community in forest plantations.

Author Contributions: Conceptualization, L.Q. and Y.W.; methodology, L.Q. and Y.W.; software, Y.W., S.X., Z.X. and J.T.; validation, L.Q. and Y.W.; formal analysis, L.Q.; investigation, L.Q. and A.M.; writing—original draft preparation, L.Q. and Y.W.; writing—review and editing, L.Q. and Y.W.; funding acquisition, L.Q. and L.T. All authors have read and agreed to the published version of the manuscript.

Funding: This research was funded by the National Natural Science Foundation of China (No. 31560109) and the Guangxi Natural Science Foundation of Guangxi Province (No. 2016JJA130091).

Data Availability Statement: The soil physicochemical data presented in this study are available on request from the corresponding author. All 16S rRNA gene sequencing data from this study are available in NCBI SRA under the study accession number PRJNA886117.

Conflicts of Interest: The authors declare no conflict of interest.

References

1. Eilers, K.G.; Debenport, S.; Anderson, S.; Fierer, N. Digging deeper to find unique microbial communities: The strong effect of depth on the structure of bacterial and archaeal communities in soil. *Soil Biol. Biochem.* **2012**, *50*, 58–65. [\[CrossRef\]](#)
2. Li, X.; Sun, J.; Wang, H.; Li, X.; Wang, J.; Zhang, H. Changes in the soil microbial phospholipid fatty acid profile with depth in three soil types of paddy fields in China. *Geoderma* **2017**, *290*, 69–74. [\[CrossRef\]](#)
3. Fierer, N.; Lef, J.W.; Adams, B.J.; Nielsen, U.N.; Bates, S.T.; Lauber, C.L.; Owens, S.; Gilbert, J.A.; Wall, D.H.; Caporaso, J.G. Cross-biome metagenomic analyses of soil microbial communities and their functional attributes. *Proc. Natl. Acad. Sci. USA* **2012**, *109*, 21390–21395. [\[CrossRef\]](#) [\[PubMed\]](#)
4. Cheng, X.; Yun, Y.; Wang, H.; Ma, L.; Tian, W.; Man, B.; Liu, C. Contrasting bacterial communities and their assembly processes in karst soils under different land use. *Sci. Total Environ.* **2021**, *751*, 142263. [\[CrossRef\]](#) [\[PubMed\]](#)
5. Kim, H.M.; Lee, M.J.; Jung, J.Y.; Hwang, C.Y.; Kim, M.; Ro, H.M.; Chun, J.; Lee, Y.K. Vertical distribution of bacterial community is associated with the degree of soil organic matter decomposition in the active layer of moist acidic tundra. *J. Microbiol.* **2016**, *54*, 713–723. [\[CrossRef\]](#)
6. Wang, M.; Tian, J.; Bu, Z.; Lamit, L.J.; Chen, H.; Zhu, Q.; Peng, C. Structural and functional differentiation of the microbial community in the surface and subsurface peat of two minerotrophic fens in China. *Plant Soil* **2019**, *437*, 21–40. [\[CrossRef\]](#)
7. Xu, T.; Chen, X.; Hou, Y.; Zhu, B. Changes in microbial biomass, community composition and diversity, and functioning with soil depth in two alpine ecosystems on the Tibetan plateau. *Plant Soil* **2020**, *459*, 137–153. [\[CrossRef\]](#)
8. Fierer, N.; Schimel, J.P.; Holden, P.A. Variations in microbial community composition through two soil depth profiles. *Soil Biol. Biochem.* **2003**, *35*, 167–176. [\[CrossRef\]](#)
9. Zhao, X.; Yang, L.; Yu, Z.; Peng, N.; Xiao, L.; Yin, D.; Qin, B. Characterization of depth-related microbial communities in lake sediment by denaturing gradient gel electrophoresis of amplified 16S rRNA fragments. *J. Environ. Sci.* **2008**, *20*, 224–230. [\[CrossRef\]](#)
10. Tang, Y.; Yu, G.; Zhang, X.; Wang, Q.; Ge, J.; Liu, S. Changes in nitrogen-cycling microbial communities with depth in temperate and subtropical forest soils. *Appl. Soil Ecol.* **2018**, *124*, 218–228. [\[CrossRef\]](#)
11. Liu, R.; Zhang, Y.; Hu, X.; Wan, S.; Wang, H.; Liang, C.; Chen, F. Litter manipulation effects on microbial communities and enzymatic activities vary with soil depth in a subtropical Chinese fir plantation. *For. Ecol. Manag.* **2021**, *480*, 118641. [\[CrossRef\]](#)
12. Montoya, J.M.; Pimm, S.L.; Sole, R.V. Ecological networks and their fragility. *Nature* **2006**, *442*, 259–264. [\[CrossRef\]](#)
13. Zhou, J.; Deng, Y.; Luo, F.; He, Z.; Tu, Q.; Zhi, X. Functional molecular ecological networks. *mBio* **2010**, *1*, e00160–e00169. [\[CrossRef\]](#) [\[PubMed\]](#)
14. Deng, Y.; Jiang, Y.; Yang, Y.; He, Z.; Luo, F.; Zhou, J. Molecular ecological network analyses. *BMC Bioinf.* **2012**, *13*, 113. [\[CrossRef\]](#)
15. Ma, J.; Lu, Y.; Chen, F.; Li, X.; Xiao, D.; Wang, H. Molecular Ecological Network Complexity Drives Stand Resilience of Soil Bacteria to Mining Disturbances among Typical Damaged Ecosystems in China. *Microorganisms* **2020**, *8*, 433. [\[CrossRef\]](#)
16. Yu, H.; Xue, D.; Wang, Y.; Zheng, W.; Zhang, G.; Wang, Z.L. Molecular ecological network analysis of the response of soil microbial communities to depth gradients in farmland soils. *Microbiol. Open* **2020**, *9*, e983. [\[CrossRef\]](#)
17. Liu, S.; Yang, Y.; Wang, H. Development strategy and management countermeasures of planted forests in China: Transforming from timber-centered single objective management towards multi-purpose management for enhancing quality and benefits of ecosystem services. *Acta Ecol. Sin.* **2018**, *38*, 1–10.
18. State Forestry and Grassland Administration. *China Forest Resources Report (2014–2018)*; China Forestry Press: Beijing, China, 2020.
19. Wan, X.; Huang, Z.; He, Z.; Yu, Z.; Wang, M.; David, R.M.; Yang, Y. Soil C: N ratio is the major determinant of soil microbial community structure in subtropical coniferous and broadleaf forest plantations. *Plant Soil* **2015**, *387*, 103–116. [\[CrossRef\]](#)
20. You, Y.; Xu, H.; Wu, X.; Zhou, X.; Tan, X.; Li, M.; Wen, Y.; Zhu, H.; Cai, D.; Huang, X. Native broadleaf tree species stimulate topsoil nutrient transformation by changing microbial community composition and physiological function, but not biomass in subtropical plantations with low P status. *For. Ecol. Manag.* **2020**, *477*, 118491. [\[CrossRef\]](#)
21. He, Y.; Qin, L.; Li, Z.; Liang, X.; Shao, M.; Tan, L. Carbon storage capacity of monoculture and mixed-species plantations in subtropical China. *For. Ecol. Manag.* **2013**, *295*, 193–198. [\[CrossRef\]](#)
22. Wang, H.; Liu, S.R.; Mo, J.M.; Wang, J.X.; Makeschin, F.; Wolff, M. Soil organic carbon stock and chemical composition in four plantations of indigenous tree species in subtropical China. *Ecol. Res.* **2010**, *25*, 1071–1079. [\[CrossRef\]](#)
23. Wang, H.; Liu, S.; Wang, J.; Shi, Z.; Lu, L.; Zeng, J.; Ming, A.; Tang, J.; Yu, H. Effects of tree species mixture on soil organic carbon stocks and greenhouse gas fluxes in subtropical plantations in China. *For. Ecol. Manag.* **2013**, *300*, 4–13. [\[CrossRef\]](#)
24. Lu, R. *Methods for Agrochemical Analysis of Soil*; China Agricultural Science and Technology Press: Beijing, China, 2000.
25. Zhou, J.; Deng, Y.; Luo, F.; He, Z.; Yang, Y. Phylogenetic molecular ecological network of soil microbial communities in response to elevated CO₂. *Mbio* **2011**, *2*, e0012211. [\[CrossRef\]](#)

26. Langille, M.G.; Zaneveld, J.; Caporaso, J.G.; McDonald, D.; Knights, D.; Reyes, J.A.; Clemente, J.C.; Burkepille, D.E.; Vega Thurber, R.L.; Knight, R.; et al. Predictive functional profiling of microbial communities using 16S rRNA marker gene sequences. *Nat. Biotechnol.* **2013**, *31*, 814–821. [\[CrossRef\]](#) [\[PubMed\]](#)
27. Olesen, J.M.; Bascompte, J.; Dupont, Y.L.; Jordano, P. The modularity of pollination networks. *Proc. Natl. Acad. Sci. USA* **2007**, *104*, 19891–19896. [\[CrossRef\]](#)
28. Louca, S.; Parfrey, L.W.; Doebeli, M. Decoupling function and taxonomy in the global ocean microbiome. *Science* **2016**, *353*, 1272–1277. [\[CrossRef\]](#)
29. Sansupa, C.; Wahdan, S.F.M.; Hossen, S.; Disayathanoowat, T.; Wubet, T.; Purahong, W. Can we use functional annotation of prokaryotic taxa (FAPROTAX) to assign the ecological functions of soil bacteria? *Appl. Sci.* **2021**, *11*, 688. [\[CrossRef\]](#)
30. Layeghifard, M.; Hwang, D.M.; Guttman, D.S. Disentangling interactions in the microbiome: A network perspective. *Trends Microbiol.* **2017**, *25*, 217–228. [\[CrossRef\]](#) [\[PubMed\]](#)
31. Mundra, S.; Kjonaas, O.J.; Morgado, L.N.; Krabberod, A.K.; Ransedokken, Y.; Kausrud, H. Soil depth matters: Shift in composition and inter-kingdom co-occurrence patterns of microorganisms in forest soils. *FEMS Microbiol. Ecol.* **2021**, *97*, fiab022. [\[CrossRef\]](#)
32. Morrien, E.; Hannula, S.E.; Snoek, L.B.; Helmsing, N.R.; Zweers, H.; de Hollander, M.; Soto, R.L.; Bouffaud, M.L.; Buee, M.; Dimmers, W.; et al. Soil networks become more connected and take up more carbon as nature restoration progresses. *Nat. Commun.* **2017**, *8*, 14349. [\[CrossRef\]](#)
33. Wagg, C.; Schlaeppli, K.; Banerjee, S.; Kuramae, E.E.; van der Heijden, M.G.A. Fungal-bacterial diversity and microbiome complexity predict ecosystem functioning. *Nat. Commun.* **2019**, *10*, 4841. [\[CrossRef\]](#)
34. Gu, Y.; Wang, Y.; Lu, S.; Xiang, Q.; Yu, X.; Zhao, K.; Zou, L.; Chen, Q.; Tu, S.; Zhang, X. Long-term fertilization structures bacterial and archaeal communities along soil depth gradient in a paddy soil. *Front. Microbiol.* **2017**, *8*, 1516. [\[CrossRef\]](#)
35. de Menezes, A.B.; Richardson, A.E.; Thrall, P.H. Linking fungal-bacterial co-occurrences to soil ecosystem function. *Curr. Opin. Microbiol.* **2017**, *37*, 135–141. [\[CrossRef\]](#)
36. Bai, R.; Wang, J.T.; Deng, Y.; He, J.Z.; Feng, K.; Zhang, L.M. Microbial community and functional structure significantly varied among distinct types of paddy soils but responded differently along gradients of soil depth layers. *Front. Microbiol.* **2017**, *8*, 945. [\[CrossRef\]](#)
37. Delgado-Baquerizo, M.; Eldridge, D.J.; Hamonts, K.; Reich, P.B.; Singh, B.K. Experimentally testing the species-habitat size relationship on soil bacteria: A proof of concept. *Soil Biol. Biochem.* **2018**, *123*, 200–206. [\[CrossRef\]](#)
38. An, Q.; Xu, M.; Zhang, X.; Jiao, K.; Zhang, C. Soil bacterial community composition and functional potentials along the vertical vegetation transection on Mount Segrila, Tibaet, China. *Chin. J. Appl. Ecol.* **2021**, *32*, 2147–2157.
39. Ahamed Bakeri, S.; Thakib Maidin, M.S.; Mohd Masri, M.M. Soil bacterial biodiversity in development of secondary loggedover forest to oil palm plantation in mineral soil of Belaga, Sarawak. *J. Oil Palm Res.* **2019**, *31*, 394–411. [\[CrossRef\]](#)
40. Jurado, M.; Lopez, M.J.; Suarez-Estrella, F.; Vargas-Garcia, M.C.; Lopez-Gonzalez, J.A.; Moreno, J. Exploiting composting biodiversity: Study of the persistent and biotechnologically relevant microorganisms from lignocellulose-based composting. *Bioresour. Technol.* **2014**, *162*, 283–293. [\[CrossRef\]](#)
41. Kirby, R. Actinomycetes and lignin degradation. *Adv. Appl. Microbiol.* **2005**, *58*, 125–168.
42. Kramer, C.; Gleixner, G. Soil organic matter in soil depth profiles: Distinct carbon preferences of microbial groups during carbon transformation. *Soil Biol. Biochem.* **2008**, *40*, 425–433. [\[CrossRef\]](#)
43. Yang, L.; Barnard, R.; Kuzyakov, Y.; Tian, J. Bacterial communities drive the resistance of soil multifunctionality to land-use change in karst soils. *Eur. J. Soil Biol.* **2021**, *104*, 103313. [\[CrossRef\]](#)
44. Øvreås, L.; Torsvik, V. Microbial diversity and community structure in two different agricultural soil communities. *Microb. Ecol.* **1998**, *36*, 303–315. [\[CrossRef\]](#)
45. Chu, H.; Sun, H.; Tripathi, B.M.; Adams, J.M.; Huang, R.; Zhang, Y.; Shi, Y. Bacterial community dissimilarity between the surface and subsurface soils equals horizontal differences over several kilometers in the western Tibetan Plateau. *Environ. Microbiol.* **2016**, *18*, 1523–1533. [\[CrossRef\]](#)
46. Ma, Y.; Feng, C.; Wang, Z.; Huang, C.; Huang, X.; Wang, W.; Yang, S.; Fu, S.; Chen, H. Restoration in degraded subtropical broadleaved forests induces changes in soil bacterial communities. *Glob. Ecol. Conserv.* **2021**, *30*, e01775. [\[CrossRef\]](#)
47. Li, X.; Zhang, Q.; Ma, J.; Yang, Y.; Wang, Y.; Fu, C. Flooding irrigation weakens the molecular ecological network complexity of soil microbes during the process of dryland-to-paddy conversion. *Int. J. Environ. Res. Public Health* **2020**, *17*, 561. [\[CrossRef\]](#) [\[PubMed\]](#)
48. Cheng, J.; Zhao, M.; Cong, J.; Qi, Q.; Xiao, Y.; Cong, W.; Deng, Y.; Zhou, J.; Zhang, Y. Soil pH exerts stronger impacts than vegetation type and plant diversity on soil bacterial community composition in subtropical broad-leaved forests. *Plant Soil* **2020**, *450*, 273–286. [\[CrossRef\]](#)
49. Lladó, S.; López-Mondéja, R.; Baldria, P. Forest soil bacteria: Diversity, involvement in ecosystem processes, and response to global change. *Microbiol. Mol. Biol. Rev.* **2017**, *81*, e00063-16. [\[CrossRef\]](#)
50. Almonacid-Muñoz, L.; Herrera, H.; Fuentes-Ramírez, A.; Vargas-Gaete, R.; Larama, G.; Jara, R.; Fernández-Urrutia, C.; da Silva Valadares, R.B. Tree cover species modify the diversity of rhizosphere-associated microorganisms in *nothofagus obliqua* (Mirb.) oerst temperate forests in south-central Chile. *Forests* **2022**, *13*, 756. [\[CrossRef\]](#)
51. Sun, W.; Li, Z.; Lei, J.; Liu, X. Bacterial communities of forest soils along different elevations: Diversity, structure, and functional composition with potential impacts on CO₂ emission. *Microorganisms* **2022**, *10*, 766. [\[CrossRef\]](#)

52. O'Donnell, A.G.; Seasman, M.; Macrae, A.; Waite, I.; Davies, J.T. Plants and fertilisers as drivers of change in microbial community structure and function in soils. *Plant Soil* **2001**, *232*, 135–145. [[CrossRef](#)]
53. Liang, S.; Deng, J.; Jiang, Y.; Wu, S.; Zhou, Y.; Zhu, W. Functional distribution of bacterial community under different land use patterns based on FaProTax function prediction. *Pol. J. Environ. Stud.* **2020**, *29*, 1245–1261. [[CrossRef](#)] [[PubMed](#)]
54. Brackin, R.; Robinson, N.; Lakshmanan, P.; Schmidt, S. Microbial function in adjacent subtropical forest and agricultural soil. *Soil Biol. Biochem.* **2013**, *57*, 68–77. [[CrossRef](#)]
55. Martin, J.F.; Reddy, K.R. Interaction and spatial distribution of wetland nitrogen processes. *Ecol. Modell.* **1997**, *105*, 1–21. [[CrossRef](#)]

Disclaimer/Publisher's Note: The statements, opinions and data contained in all publications are solely those of the individual author(s) and contributor(s) and not of MDPI and/or the editor(s). MDPI and/or the editor(s) disclaim responsibility for any injury to people or property resulting from any ideas, methods, instructions or products referred to in the content.